



## Assessment of the Direct Economic Losses of Flood Disasters Based on the Spatial Valuation of Land Use and Quantification of Vulnerabilities: A Case Study of the 2014 Flood in Lishui city, China

Haixia Zhang<sup>1,2</sup>, Weihua Fang<sup>1,2,3</sup>, Hua Zhang<sup>1,2</sup>

5 <sup>1</sup> Key Laboratory of Environmental Change and Natural Disaster of Ministry of Education, Faculty of Geographical Science, Beijing Normal University, Beijing 100875, China

<sup>2</sup> Academy of Disaster Risk Science, Faculty of Geographical Science, Beijing Normal University, Beijing 100875, China

<sup>3</sup> Southern Marine Science and Engineering Guangdong Laboratory, Guangzhou 511458, China

*Correspondence:* Weihua Fang (weihua.fang@bnu.edu.cn)

10 **Abstract.** The refined assessment of the direct economic losses of flood disasters is important for emergency dispatch and risk management in small- and medium-sized cities. There are still great challenges in the accuracy and timeliness of the previous research methods. In this study, a single flood disaster in Lishui city in 2014 was taken as an example to study and verify a method for the rapid and refined assessment of direct economic loss. First, based on a field investigation, the inundation range and submerged depth simulated by the flooding model were verified. Next, the urban land use status map and high-precision remote sensing classification data were fused and combined with expert questionnaire surveys, thereby providing the types and values of disaster-bearing bodies. Then, the existing vulnerability curve database was summarized, and the curves were calibrated by disaster loss reporting. Finally, the spatial distributions of the flood disaster loss ratio and loss value were estimated by spatial analysis. It is found that the constructed land use map has detailed types and value attributes as well as high-precision spatial information. Secondly, the vulnerability curves after function fitting and calibration effectively reflect the change characteristics of land use loss ratio in this area. Finally, the estimated loss ratio and loss value distributions can accurately reflect the spatial pattern of flood disaster loss, which is useful for the government to formulate effective disaster reduction and relief measures.

**Key words:** Flood disaster, Direct economic loss, Loss assessment, Vulnerability curve

### 1 Introduction

25 Refined assessments of the direct economic losses of flood disasters are very important in disaster emergency rescue and urban flood risk management (Li et al., 2017; UNISDR, 2015). The results of a rapid quantitative assessment of disaster losses with high spatial resolution not only provide suggestions for the government to formulate emergency dispatch management measures, such as releasing disaster information, deploying rescue forces and relief materials, and the emergency resettlement of disaster victims, but also lay a data foundation for decision-makers to plan sponge cities and formulate flood risk management systems and climate change adaptation policies (Alfieri et al., 2016; Merz et al., 2010).



As a key component of flood risk assessment, flood loss assessment has been extensively analyzed by researchers (Falter et al., 2015; Koks et al., 2015). The flood loss data obtained from a comprehensive high-quality field survey after a disaster can accurately reflect the disaster loss situation and has important reference value for the establishment and verification of flood loss models (Carisi et al., 2018). However, given that loss data can only be obtained after a flood, these data cannot provide  
35 timely guidance for disaster relief. Collecting loss data is also time-consuming and laborious, which supports the further development of flood loss assessment models.

Due to the development of existing flood loss assessment models, there are relatively mature methods and tools (EMA, 2002; Scawthorn et al., 2006), and the popularization of flood insurance provides relatively complete socioeconomic and disaster loss data; thus, disaster losses can be quickly assessed when floods occur (Hsu et al., 2011). The United States (Smith  
40 D, 1994), the United Kingdom (Stephenson and D' Ayala, 2013), Japan (Dutta et al., 2003), Canada (NRC, 2017), Australia (Hasanzadeh Nafari et al., 2016b, 2016a), Italy (Amadio et al., 2016), China (Li et al., 2012; Penning-Rowsell et al., 2013), and other flood-prone countries have carried out a large number of loss assessment studies using different classification systems of disaster-bearing bodies and then used the existing loss database and post-disaster investigation data to establish local flood vulnerability curves.

In addition, with the development and application of hydrological models and hydrodynamic models, geographic information systems (GISs), and remote sensing (RS) (Elkhrachy, 2015; Jonkman et al., 2008), flood loss assessment models based on depth-damage functions have been improved (Komolafe et al., 2018). However, there are still some problems. First, there is a lack of a depth-damage functions for use in specific areas, which need to be constructed through extensive post-disaster survey data (Albano et al., 2018). Second, the effect and accuracy of the assessment are affected by the scale of the  
50 disaster-bearing body. The microscale loss assessment model for each affected object (building, infrastructure object, etc.) has poor applicability. However, mesoscale disaster-bearing body data mainly refer to land use data obtained through remote sensing (RS) interpretation (Merz et al., 2010). Although mesoscale data can effectively be used to extract the spatial distribution of buildings, it is difficult to identify the use types of buildings. These problems lead to high uncertainties and disparities in flood loss assessments (Gerl et al., 2016).

With the introduction of fuzzy mathematics, gray system models, genetic algorithms, and other mathematical methods, the rapid estimation and prediction of regional flood direct economic loss can be realized (Qie and Rong, 2017; Zhao et al., 2014; Zhou et al., 2006), which can effectively reflect the overall situation of economic losses in a large region and reduce the investment in human and material resources. However, due to the lack of high-resolution spatial location information, this approach cannot provide timely and effective suggestions for the government to formulate targeted emergency scheduling  
60 plans.

To effectively improve the accuracy, timeliness, and practicability of flood disaster loss assessment, a refined assessment model of single-flood disaster losses in small- and medium-sized cities is explored in this paper. The heavy rainfall from 18 August 2014 to 20 August 2014 caused serious river backflow and urban waterlogging, and many houses and roads were flooded in Lishui city. Therefore, taking this flood disaster as an example, a refined assessment model for the direct economic

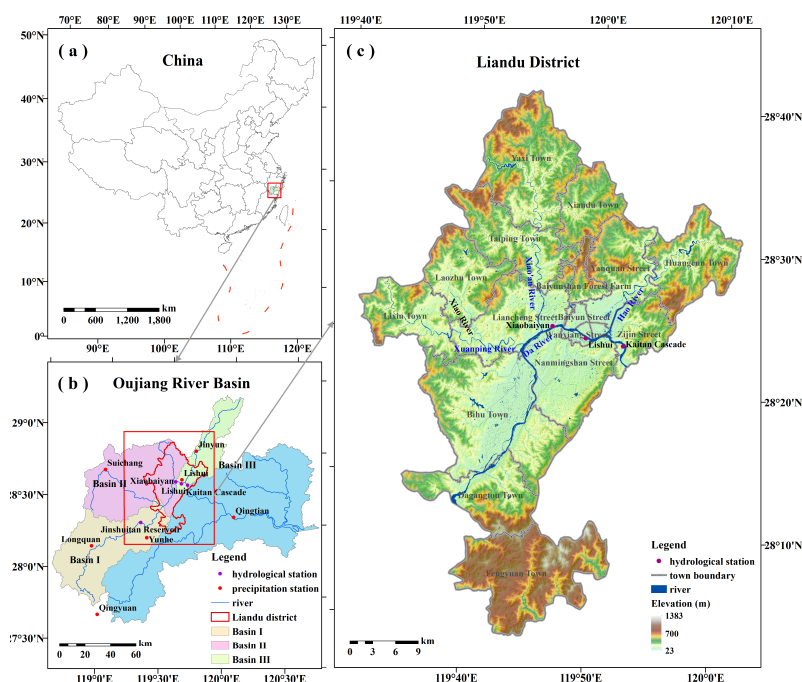




65 losses of regional flooding disasters was constructed. The model includes flood inundation models, the spatial distribution of  
land use types, the quantification of land use values, vulnerability curve fitting, and optimization, as well as loss ratio and loss  
value estimations.

## 2 Materials

### 2.1 Study area



70 **Figure 1. Location of the study area. (a. The location of Oujiang River Basin in China. b. The distribution of hydrological stations, precipitation stations, rivers and sub basins in Oujiang River Basin, and the location of Liandu District in Oujiang River Basin. c. The terrain distribution and town boundary of Liandu district.)**

75 Liandu District is in southwestern Zhejiang Province, between 28°06' N-28°44' N and 119°32' E-120°08' E (Figure 1). This district is in the middle reaches of the Oujiang River Basin, surrounded by hills and mountains with plains in the middle, spanning a total area of approximately 1,502 km<sup>2</sup>. Liandu District is situated within Lishui city, with a relatively concentrated population and socioeconomic status. As a result of both urban planning and topography, the flood disaster in Liandu District caused heavy losses. Because topography has a great impact on hydrology and hydrodynamics, it is easy to ignore regional



80 differences based on administrative units. Considering the impact of the Jinshuitan Reservoir operation, the upper reaches of the Oujiang River Basin are divided into three sub watersheds (Figure 1).

## 2.2 Precipitation

The gridded precipitation data come from the hourly precipitation data set of the National Meteorological Information Center, which integrates China's automatic station data with the NOAA CDR Climate Prediction Center morphing technique (CMORPH) product with a resolution of  $0.1^\circ$ . The overall error is within 10%, and the accuracy in areas with heavy rainfall and sparse sites is greater than in similar international products (Shen et al., 2014). The data can effectively reproduce the spatiotemporal pattern of rainfall and are suitable for simulating flood inundation.

85 Based on the hourly precipitation levels, the mean accumulated precipitation of the middle and upper reaches of the Oujiang River Basin and the 3 sub watersheds were calculated (Figure 2). The precipitation change trend of each sub watershed is generally the same, with the accumulated precipitation exceeding 210 mm. The precipitation increased rapidly after 5:00 on August 18<sup>th</sup>, and the entire precipitation process basically ended at 10:00 on August 20<sup>th</sup>.

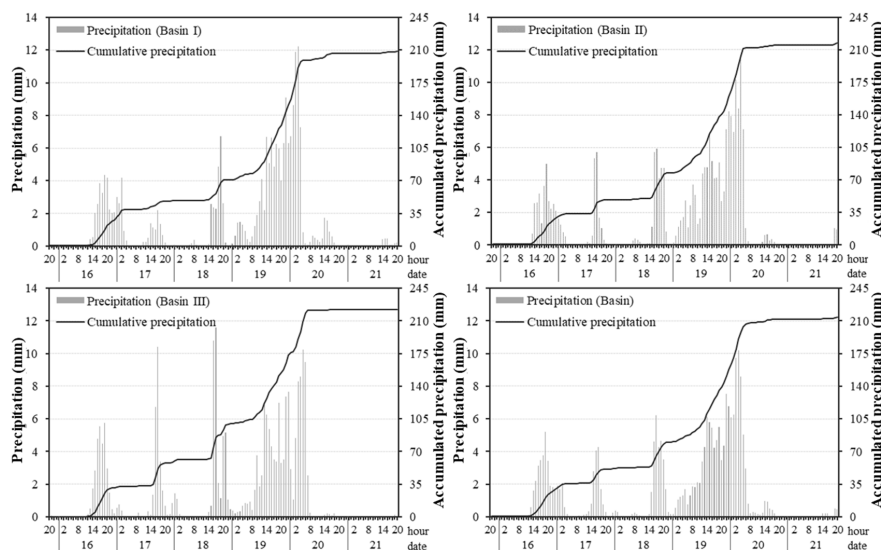


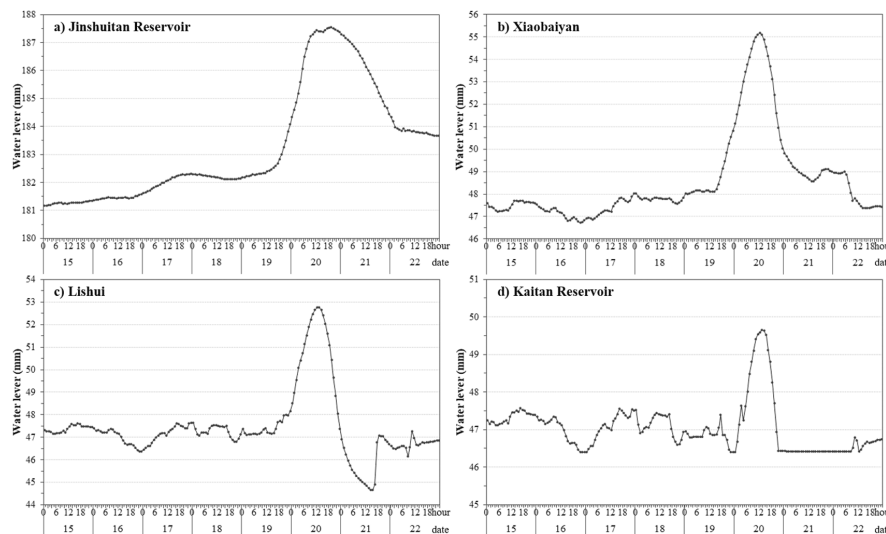
Figure 2. Distribution of hourly and accumulated precipitation in the entire basin and each subbasin. (The grey column is hourly precipitation, and the black curve is cumulative precipitation. The precipitation time is from 20:00 on August 15<sup>th</sup> to 20:00 on August 21<sup>st</sup>, 2014.)

## 95 2.3 Water level and flood inundation

The water level data come from the hourly observations of hydrological stations of the Zhejiang Water Resources Department, including the measured water level, warning water level, and guaranteed water level. Xiaobaiyan and Lishui are river stations,



and the Jinshuitan Reservoir and the Kaitan Reservoir are reservoir stations (Figure 1). Based on the hourly measured water level, beginning at 12:00 on August 19<sup>th</sup>, the water levels of the Jinshuitan Reservoir, Xiaobaiyan, and Lishui increased significantly, while the water level of the Kaitan Reservoir first dropped slightly and then increased significantly, and the water levels at these stations reached a peak at approximately 12:00 on August 20<sup>th</sup>. The water levels at Xiaobaiyan, Lishui, and the Kaitan Reservoir returned to normal at 00:00 on August 21<sup>st</sup>, while that at the Jinshuitan Reservoir dropped to a certain water level at 00:00 on August 22<sup>nd</sup>, and the subsequent downward trend was slow (Figure 3).



105 **Figure 3. Distribution of hourly water levels at hydrological stations. (The time of water level data is from 00:00 on August 15<sup>th</sup> to 00:00 on August 23<sup>rd</sup>, 2014)**

The flood inundation was calculated from the Yuxi to Kaitan Reservoir hydraulic model constructed by *Zhejiang Design Institute of Water Conservancy & Hydro-Electric Power*. The unsteady flow partial differential equations of the Saint-Venant open channel are used to construct a one-dimensional hydrodynamic model. Then, based on the measured channel section, water level, reservoir discharge, and high-precision topography, the implicit difference method and Gaussian principal component elimination method are used to solve the water level and discharge of each section, and then the parameters are calibrated by the measured water level (Kang and Chen, 2007). After multiple verifications, the difference between the measured and calculated water levels was between 0 m and 0.09 m. The flood volume was calculated based on the simulated water level and the elevation of the embankment (Table 1). When compared with the site survey and flood traces, the result is similar to the actual submerged depth.

110  
115



Based on the simulated maximum submerged depth distribution (Figure 4a) and real-time aerial photographs (Figure 4b, Figure 4c), the flood inundation area is mainly concentrated in the river confluence and both sides of the river, the submerged depth decreases from the river bank to both sides, and the submerged depth of the central island is generally greater than 7 m.

**Table 1. Overflow volume of Liandu District in 2014 based on the hydraulic model (10,000 m<sup>3</sup>)**

|                        | Da River South | Da River East | Da River North (Da River Section) | Da River North (Hao River Section) |
|------------------------|----------------|---------------|-----------------------------------|------------------------------------|
| <b>Overflow volume</b> | 230.63         | 264.81        | 60.17                             | 277.51                             |

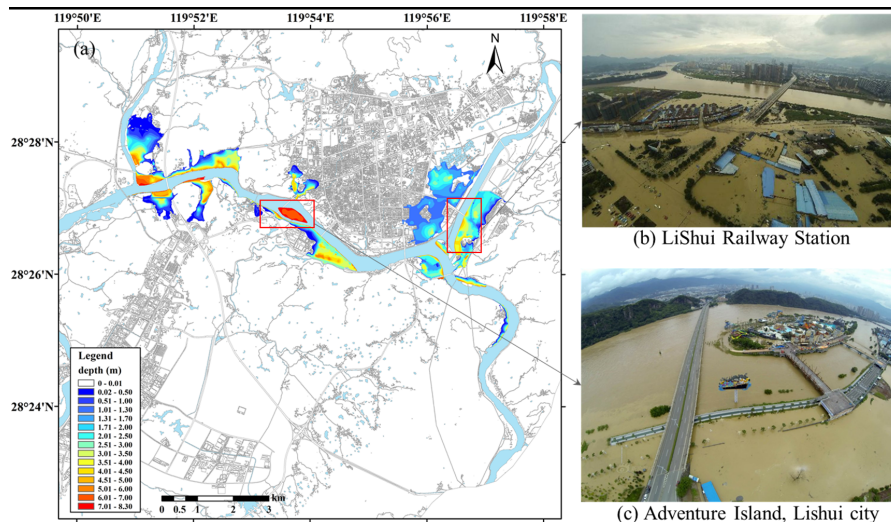


**Figure 4. (a) Maximum simulated submergence depth distribution, (b, c) Aerial photographs of Liandu District in 2014.**

#### 2.4 Disaster loss reporting

The disaster loss report is obtained from the Lishui Civil Affairs Bureau and is conveyed by the local government. The report records 41 statistical indicators, including the affected population, affected area of crops, agricultural losses, infrastructure losses, public welfare facility losses, household property losses, and direct economic losses. According to these statistics, a total of 167,300 people were affected in Liandu, 17,330 people were relocated in emergencies, 247 rural houses collapsed, and the direct economic loss was approximately 377.15 million yuan.

The insurance claim data come from the auto insurance list of the catastrophe "Zhejiang 0819 Rainstorm" of the Lishui branch of the People's Insurance Company of China (PICC), and the data record 19 indicators, including the policy number, the information of the insured, the estimated compensation, and the compensation paid. As of August 24<sup>th</sup>, a total of 1,045 motor vehicle insurance reports were received, with a reported loss of 50.7969 million yuan and a decided compensation of



50.6893 million yuan. According to the analysis of the market share of various insurance types in Zhejiang Province in December 2014, PICC motor vehicle insurance accounted for approximately 48.357% of Lishui city.

### 3 Methods

135 In this study, an assessment model of the direct economic loss ratio and loss value of flood disasters was constructed by utilizing methods such as land use type fusion, land use value estimation, vulnerability curve fitting, and optimization.

#### 3.1 Data fusion of land use types

The distribution of land use types is obtained through the fusion of current land use data in Lishui city with a high-precision remote sensing classification. The former data come from the urban and rural space development current status map of the Natural Resources and Planning Bureau in 2013, which is divided into 47 categories according to the *Urban Land Classification and Planning and Construction Land Standards* (GB 50137-2011, 2011). The remote sensing classification is derived from the Gaode map with a resolution of 2.3870768 m, including 5 categories: transportation, grassland, waters, agriculture and forest, and buildings. The steps of vector and raster fusion are as follows.

145 1) The unified coordinate system is adopted, the nearest neighbor method is used to resample the data onto a grid with a spatial resolution of 2 m, and geometric correction and spatial registration are performed on the vectorized land use data.

2) The building pixels in the remote sensing classification are traversed, the corresponding current land type is queried by the location, and the grid is reassigned using the type. The building pixels that have not been reassigned are assigned according to the adjacent building types. In addition, the road within 2 m of the residence is set as community parking, and buildings far from urban areas are set as rural residences.

150 3) The water, agriculture and forest, and road in the remote sensing classification are assigned as water, agriculture and forest, and urban road, respectively. The agriculture and forest in areas with urban buildings and the agriculture and forest and grassland in park areas are assigned as park green land.

4) Whether there are pixels in the remote sensing classification that have not been reassigned is checked. If so, the corresponding current land type is determined, and all pixels are classified.

#### 155 3.2 Estimation of land use values

The value of land use obtained from expert questionnaires is relatively reliable, and the steps are as follows.

1) Based on the *Lishui Master Plan (2013-2030)*, *Lishui 13<sup>th</sup> Five-Year Plan*, and *Lishui Statistical Yearbook in 2015*, reference information such as current area, planned area, planned investment, unit area budget, and description of land use types are given.

160 2) As to the characteristics of land use, the four major categories of residential, commercial, industrial, public management, and public services are used to estimate the value of indoor properties, and the cost per unit area is estimated for others.



3) Questionnaires are issued to 7 experts in fields such as municipal engineering design, construction industry, water design, ecological city planning, and natural disasters, and experts are invited to estimate the land use value based on their professional background knowledge and the actual situation of the study area.

165 4) The value of each land use is determined by collating the questionnaires and calculating the average values.

### 3.3 Calibration of vulnerability curves

Although the vulnerability curves of different regions are different, there are similarities in the trend of the loss ratio with the water depth, which we can learn from. Therefore, based on the existing vulnerability curves in many countries and regions (Coto, 2002; Dutta et al., 2003; FEMA, 2017; Mo and Fang, 2016; NRC, 2017; Reese and Ramsay, 2010; Shi, 2010; Wehner et al., 2017), the steps of vulnerability curve fitting are as follows.

170 1) The relationship between the flooding depth and loss ratio is formulated in Liandu based on existing databases. HAZUS-Flood has a relatively complete classification, so a mapping table between the database and land use type of Liandu is established. The average loss ratio of the corresponding type of HAZUS functions as a reference for the loss ratio of Liandu. If there is no similar type in HAZUS, other databases are referenced.

175 2) The vulnerability curve can be fitted by a polynomial, a power function (Büchele et al., 2006), or logistic regression (Cao et al., 2016), and it can also be smoothed by nonparametric forms such as the kernel density (Merz et al., 2004). The lognormal cumulative distribution function (Limpert et al., 2001) with a high fitting degree is selected to fit the vulnerability curve, and the formula is as follows:

$$y = F(x|\mu, \sigma) = \frac{1}{\sigma\sqrt{2\pi}} \int_0^x \frac{1}{t} e^{-\frac{(\log t - \mu)^2}{2\sigma^2}} dt, \quad x > 0 \quad (1)$$

180 where  $F$  is the direct economic loss ratio,  $x$  is the submerged depth, and  $\sigma$  and  $\mu$  are the standard deviation and mean of the logarithm of  $x$ , respectively.

3) Based on the fitted vulnerability curve of land use, the loss ratio is calculated by the two attributes of the submerged depth and land use type. Then, the loss value is calculated based on the loss ratio and land use value, and the formula is as follows:

$$L = DR * V \quad (2)$$

185 where  $L$  is the loss value of the land use,  $DR$  is the loss ratio of the land use, and  $V$  is the value of the land use.

4) Based on the mapping relationships between the disaster statistical indicators and land use types, the simulated direct economic losses are summarized, and the nonlinear equation is established with the minimum error of the disaster statistical loss and the simulated loss as the objective function. The least square method is used to solve the nonlinear equation to optimize the scale parameters, and then the optimized vulnerability curve is used to re-estimate the disaster loss.

## 190 4 Results and Analysis

### 4.1 Distribution of land use types



The distribution of high-resolution land use types in Liandu is obtained by implementing the data fusion method (Figure 5a), and the names and codes of land use types are shown in Table 2. The data effectively integrate the corresponding advantages of the current urban land use and remote sensing classification. The data not only have high-resolution spatial location information but also reflect the detailed types of land use.

Agricultural and forestry land in Liandu District is the most widely distributed type. Woodlands are mainly distributed in the hilly areas of the north, east, south, and northeast. The built-up area of Liandu District is distributed along the river in a block shape, among which residential land is mainly distributed in communities near the river. Industrial land is mainly distributed in northeastern Wanxiang Street and the Economic and Technological Development Zone, which is currently in the development stage, and many industrial plants have been built.

To strengthen intraregional connections, the roads and traffic facilities are relatively complete, with an urban road area of 4.33 km<sup>2</sup>. Commercial, warehouse, public management, and public service facilities are relatively small and scattered. They are mainly concentrated near residential and industrial land, providing various services. Park green space is distributed along the river or close to residential and commercial land, while square green space, protective green space, and public facilities are small and scattered.

#### 4.2 Distribution of land use values

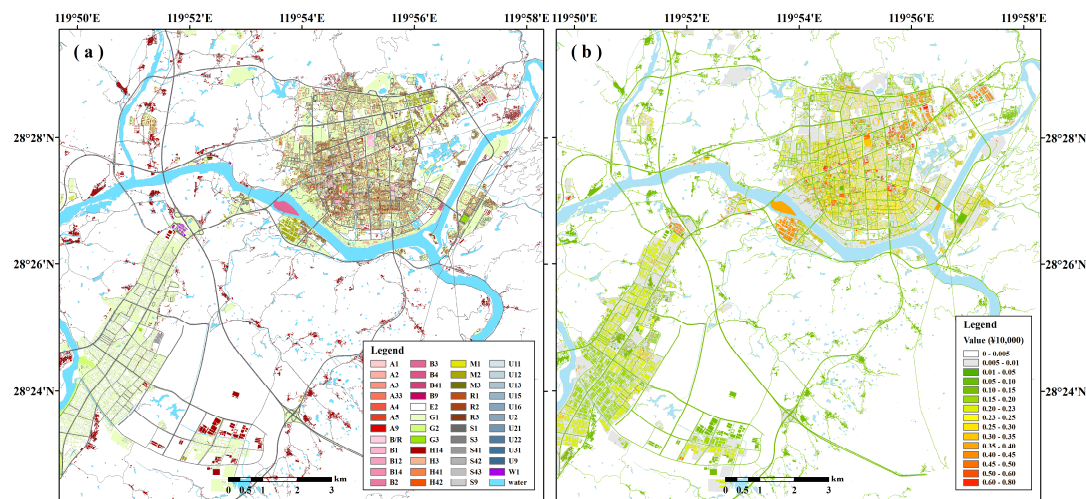


Figure 5. Distribution of land use types (a) and land use values (b) in the central urban area of Liandu District in 2013.

The asset value or cost per unit area of land use types is estimated based on expert questionnaires (Table 2). Commercial and industrial land has many internal equipment and items with the highest asset unit price. Public management and public service facilities and residential land have a higher indoor property value. The value of agricultural and forestry land is the lowest.





The spatial distribution of land use value in Liandu in 2013 is calculated through grid assignment (Figure 5b). The value of assets per unit area in the northern city and Wanxiang Street is generally high due to the concentration of commercial, industrial, residential, public management, and public service facilities in the area. There is a water amusement project on the central island, which has a higher value per unit area. Many industrial plants are distributed in the Economic and Technological Development Zone, but due to the development stage and incomplete internal facilities, the unit price of the industrial land in this zone is calculated at half of the estimated value. Agricultural and forestry land is widely distributed and low in value, so most areas of Liandu have low values.

#### 4.3 Fitted vulnerability curves

The vulnerability curves of all land use types are fitted by a lognormal cumulative distribution function based on the matrix of the submerged depth and loss ratio. By comparing the simulated losses and disaster loss reporting (Table 2), the scale parameter of the vulnerability curve is optimized through the least square method (Figure 6).

The loss ratios of residential, industrial, commercial, warehousing, public management, and public service land are very high, mainly due to indoor properties being soaked or washed away by floods. As the submerged depth increases, the loss ratio increases rapidly. When the depth is higher than 3 m, the loss ratio increases, and the rate of increase is unclear.

**Table 2 The Classification, value, inundated area of land use types, and the comparison of simulated loss before optimization, simulated loss after optimization and statistics loss of each land use type in Liandu District.**

| Code | Classification                        | Value (¥10,000/4 m <sup>2</sup> ) | Total value (¥10,000) | Inundated area (m <sup>2</sup> ) | Mean loss ratio of inundated area | Simulation loss before optimization (¥10,000) | Simulation loss after optimization (¥10,000) | Statistical loss (¥10,000) |
|------|---------------------------------------|-----------------------------------|-----------------------|----------------------------------|-----------------------------------|---|--|----------------------------|
| A1   | administrative office                 | 0.40                              | 13891.60              | 2020                             | 0.79                              | 160.41  | 130.81                                       |                            |
| A2   | cultural facilities                   | 0.35                              | 3309.60               | 24                               | 0.81                              | 1.71  | 1.13   |                            |
| A3   | educational and scientific research   | 0.25                              | 13914.00              | 15980                            | 0.64                              | 639.38  | 499.98                                       |                            |
| A33  | primary and secondary schools         | 0.20                              | 5946.60               | 7296                             | 0.31                              | 111.98  | 77.36  | 741                        |
| A4   | sports land                           | 0.30                              | 1311.45               | 0                                | 0.00                              | 0.00  | 0.00   |                            |
| A5   | medical and health land               | 0.35                              | 4601.27               | 568                              | 0.80                              | 39.82   | 31.72  |                            |
| A9   | religious land                        | 0.10                              | 288.70                | 0                                | 0.00                              | 0.00  | 0.00   |                            |
| B/R  | commercial and residential land       | 0.35                              | 8415.99               | 144                              | 0.45                              | 5.66  | 1.87   |                            |
| B1   | commercial facilities                 | 0.46                              | 9944.74               | 5908                             | 0.89                              | 602.53  | 473.27                                       |                            |
| B12  | wholesale market land                 | 0.50                              | 15358.25              | 16252                            | 0.48                              | 981.98  | 457.98                                       |                            |
| B14  | hotel land                            | 0.30                              | 3247.50               | 2520                             | 0.29                              | 54.51   | 19.38  | 2940                       |
| B2   | business facilities                   | 0.60                              | 11071.80              | 1100                             | 0.10                              | 16.17   | 2.00   |                            |
| B4   | business outlets of public facilities | 0.35                              | 18.55                 | 148                              | 0.47                              | 6.15  | 3.20   |                            |
| B41  | gas station                           | 0.44                              | 249.70                | 0                                | 0.00                              | 0.00  | 0.00   |                            |





|     |                                    |       |            |         |      |          |          |       |
|-----|------------------------------------|-------|------------|---------|------|----------|----------|-------|
| B9  | other service facilities           | 0.23  | 350.06     | 2308    | 0.64 | 84.37    | 48.19    |       |
| M1  | class I industrial                 | 0.60  | 20913.60   | 336     | 0.81 | 40.92    | 30.04    |       |
| M2  | class II industrial                | 0.40  | 146229.20  | 32592   | 0.52 | 1692.03  | 1059.57  |       |
| M3  | class III industrial               | 0.30  | 39283.50   | 10132   | 0.55 | 418.00   | 237.72   |       |
| W1  | Warehouse                          | 0.50  | 7500.00    | 7904    | 0.85 | 836.18   | 606.79   |       |
| E2  | agriculture and forest             | 0.004 | 1398391.70 | 3943224 | 0.65 | 637.25   | 637.25   | 5506  |
| R1  | class I residential                | 0.35  | 3312.05    | 0       | 0.00 | 0.00     | 0.00     |       |
| R2  | class II residential               | 0.25  | 104612.25  | 232924  | 0.53 | 7666.89  | 9435.06  |       |
| R3  | class III residential              | 0.20  | 35893.50   | 78672   | 0.70 | 2756.77  | 3189.11  | 25080 |
| H14 | village construction               | 0.13  | 425820.70  | 176868  | 0.78 | 4507.90  | 5189.18  |       |
| S43 | community parking                  | 0.50  | 63235.50   | 66468   | 0.75 | 6191.58  | 7266.65  |       |
| H3  | regional public facilities         | 0.15  | 349.80     | 0       | 0.00 | 0.00     | 0.00     |       |
| H41 | military sites                     | 0.30  | 629.70     | 0       | 0.00 | 0.00     | 0.00     |       |
| H42 | security                           | 0.08  | 467.60     | 0       | 0.00 | 0.00     | 0.00     |       |
| S1  | urban road                         | 0.12  | 1055377.42 | 931240  | 0.07 | 2047.78  | 2141.03  |       |
| S3  | transportation hub                 | 0.28  | 5559.96    | 4592    | 0.08 | 25.16    | 26.12    |       |
| S41 | public transport station           | 0.40  | 0.80       | 0       | 0.00 | 0.00     | 0.00     |       |
| S42 | social parking                     | 0.60  | 2106.60    | 0       | 0.00 | 0.00     | 0.00     |       |
| S9  | other transportation facilities    | 0.15  | 284.70     | 4       | 0.44 | 0.07     | 0.07     |       |
| U11 | water supply                       | 0.27  | 857.25     | 0       | 0.00 | 0.00     | 0.00     |       |
| U12 | power supply                       | 0.30  | 930.90     | 8       | 0.06 | 0.04     | 0.04     | 3448  |
| U13 | gas supply                         | 0.40  | 108.40     | 0       | 0.00 | 0.00     | 0.00     |       |
| U15 | communication facilities           | 0.80  | 3294.40    | 0       | 0.00 | 0.00     | 0.00     |       |
| U16 | radio and television facilities    | 0.80  | 808.80     | 0       | 0.00 | 0.00     | 0.00     |       |
| U2  | environmental facilities           | 0.50  | 140.50     | 0       | 0.00 | 0.00     | 0.00     |       |
| U21 | drainage facilities                | 0.45  | 757.35     | 3352    | 0.25 | 94.22    | 96.50    |       |
| U22 | sanitation facilities              | 0.15  | 197.40     | 544     | 0.17 | 3.44     | 3.53     |       |
| U31 | fire control facilities            | 0.30  | 727.20     | 0       | 0.00 | 0.00     | 0.00     |       |
| U9  | other public facilities            | 0.15  | 21.00      | 0       | 0.00 | 0.00     | 0.00     |       |
| G2  | protection greenbelt               | 0.01  | 713.15     | 0       | 0.00 | 0.00     | 0.00     |       |
| G3  | square land                        | 0.08  | 1178.96    | 28192   | 0.41 | 230.11   | 233.69   |       |
| G1  | park green space                   | 0.01  | 48264.89   | 1608096 | 0.55 | 2211.92  | 2211.92  |       |
| B3  | recreational and sports facilities | 0.38  | 18234.68   | 161216  | 0.88 | 13540.95 | 13540.95 |       |

The direct impact of floods on public facilities and roads is relatively small, and the loss ratio is generally low. However, the indirect loss caused by the suspension of roads, communications, and electricity is relatively large but is not calculated in this study. Green space and square land are less affected by floods, and the loss ratio is relatively low.

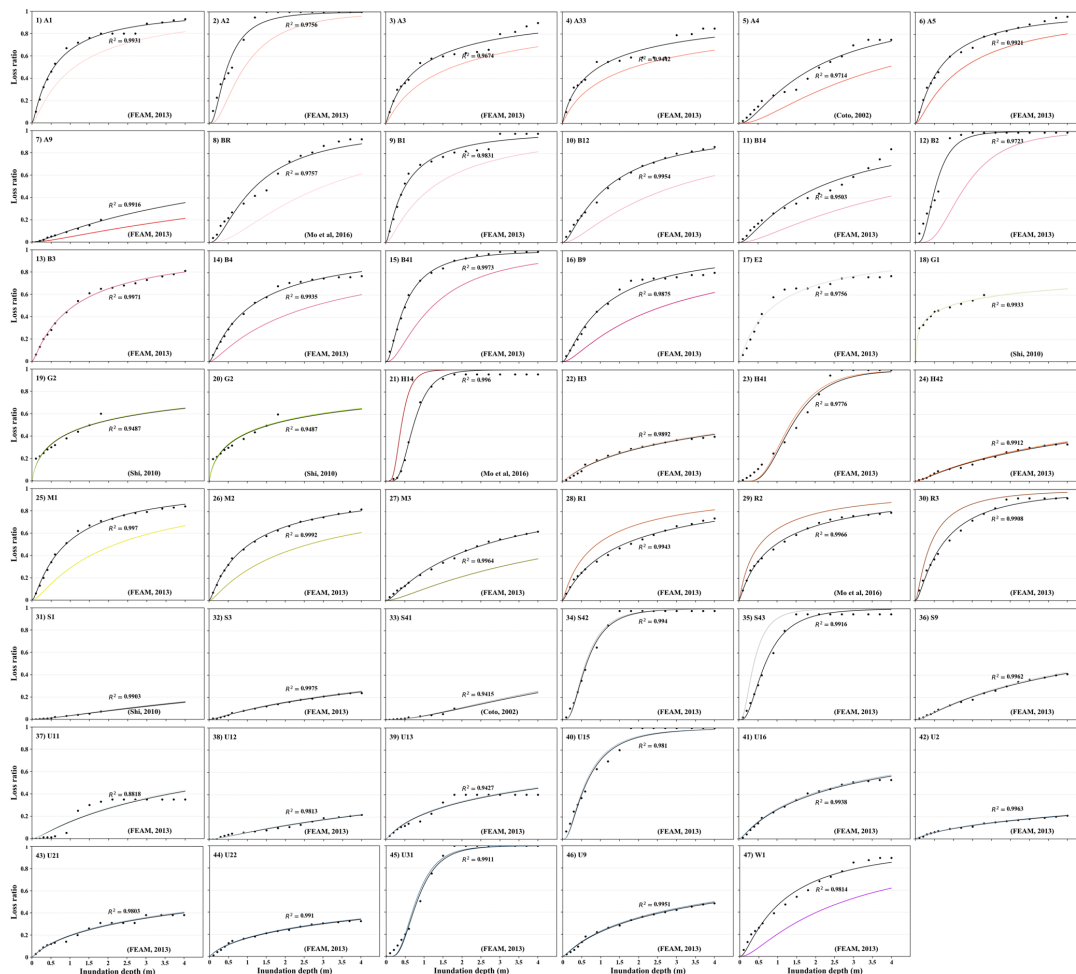


**Figure 6. Fitting and optimization of vulnerability curves of land use in Liandu District (The black curve is the fitting result, and the color curve is the optimized result).**

235 The same optimization coefficients are selected for the scale parameters of the same type of land use vulnerability curve and are obtained by solving nonlinear equations. The vulnerability curve of family property is stretched, that of infrastructure is stretched slightly, and those of public welfare facilities, industry, and commerce shrink. This comparison shows that the simulated loss after optimization is consistent with the disaster loss reporting, and the optimization effect is good (Table 2).

#### 4.4 Distributions of the loss ratio and loss value



240 The loss ratio (Figure 7a) and loss value (Figure 7b) distributions of the flood disaster in Liandu District are obtained based on a spatial analyst algorithm.

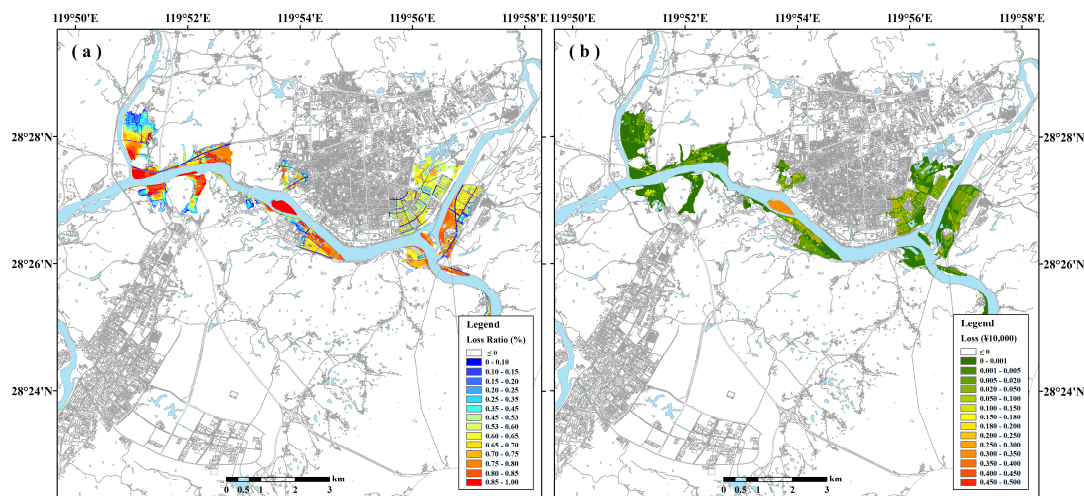


Figure 7. Spatial distribution of the flood loss ratio (a) and loss values (b) in the central urban area of Liandu District in 2014.

245 Due to the high inundation depth at the river confluence and both sides of the river as well as the wide distribution of agricultural land in the area, the mean loss ratio of these areas is approximately 0.63. The submerged depth of the island is more than 7 m, and there are entertainment facilities on it, so the loss ratio is more than 0.6. In addition, the submerged depth on both sides of the Hao River is more than 1 m. The west side of the river is mainly residential land, and the east side is the Lishui railway station, so the indoor property loss ratio is high. However, traffic land is less directly affected by floods, so the loss ratio is less than 0.2 (Figure 7a).

250 The loss value of a flood disaster is affected by the unit value and loss ratio of the land use. Therefore, the distribution characteristics of the loss rate and loss value are different. The loss ratio of this flood is relatively high, but due to the wide distribution of agricultural land in the submerged area, the loss value per unit area is low. The loss ratio and unit area value of recreational and sports facilities, residential, industrial, commercial, public management, and public service facilities are high, so the loss values are also high. The loss ratio of traffic facilities is very low, yet the loss value is relatively high due to the high construction cost (Figure 7b).

255 Liandu District is surrounded by high mountains, and the overland flow, affected by the topography, was formed by rainfall flowing into the Da River through the rivers in the north. The occurrences of heavy rainfall in the middle and upper reaches of the Oujiang River are similar, causing the whole basin to experience the flood peak period at the same time, which is not conducive to flood diversion efforts. To relieve the flood pressure on the basin, the Jinshuitan Reservoir was opened twice. At the same time, rapid urbanization has brought about great changes in the morphology of river channels and waters. These



260 factors caused the river's water level to rise rapidly, overtopping the flood dyke and submerging low-lying areas along the  
riverbed. In addition, due to the high population density and highly concentrated economy in the northern area of Liandu  
District, serious economic losses will inevitably occur when floods exceed the fortification standard.

## 5 Conclusion and discussion

The research and verification of the refined assessment of single-flood disaster loss was carried out by utilizing the refined  
265 types and values of land use and quantitative vulnerability curves, and the main conclusions are as follows.

The land use type data obtained by the fusion of vector and raster data overcome the limitations of the original data. This  
procedure not only refines the data into detailed urban land use types but also has a high spatial resolution. In addition, the unit  
area costs or asset values obtained through the collection of written sources and a survey of experts via a questionnaire are  
more reasonable. The land use types and values constructed by the above methods provide fine and reasonable disaster-bearing  
270 body data for a refined assessment of disaster losses, thus laying a data foundation.

Based on lognormal cumulative distribution function fitting and scale parameter optimization, the vulnerability curves of  
47 types of disaster-bearing bodies accurately reflect the characteristics of the loss ratio of the disaster-bearing bodies varying  
with the submerged depth in Liandu District and provide a reliable stage damage function curve for refined loss assessment.  
Among these disaster-bearing bodies, residential, industrial, commercial, public management, and storage land are seriously  
275 affected by flooding. Other land uses are relatively less affected, and the loss ratio increases slowly. In the absence of a large  
amount of post-disaster field survey data, the method proposed in this study can be used to construct vulnerability curves in  
accordance with the regional situation.

A refined assessment model of the direct economic loss of a single flood disaster is constructed in accordance with the  
regional characteristics based on the refined research and verification of each link in the disaster loss assessment. The estimated  
280 spatial distributions of the loss ratio and loss value of the flood disaster accurately reflect the spatial pattern of disaster loss  
and provide scientific guidance for disaster prevention, mitigation, and emergency rescue. In addition to park green space,  
recreational and sports facilities, and agricultural and forestry land, the losses of other land use types after optimization are  
consistent with the loss reporting, indicating that the loss assessment model of this study can be effectively applied to this area.

The loss assessment model constructed in this study can be used to estimate flood disaster losses under different climate  
285 change and economic development scenarios, providing a basis for flood risk assessment and management in small- and  
medium-sized cities. This, in turn, will help the government formulate reasonable climate adaptation policies and sponge city  
planning.

In this study, only the inundation and disaster loss reporting of one precipitation event are collected, thereby affecting, to a  
certain extent, the optimization results of the vulnerability curves. In the future, the data of several precipitation events will be  
290 collected to better calibrate the vulnerability curves and render the final optimized vulnerability curves more suitable for the  
region. Furthermore, the flood disaster caused serious direct economic losses to Liandu District. The disaster also stimulated



a large amount of disaster relief investment, even as it disrupted public services and traffic, caused production losses for companies outside the flooded area, reduced agricultural production, and affected related industries (Jonkman et al., 2008). Therefore, it is necessary to carry out further research regarding the refined assessment of the indirect economic losses of flood disasters.

**Code and data availability.** The data used in the study are available at <https://github.com/Haixia-Zhang/Flood-loss-assessment.git>

**Author contributions.** ZHX and FWH conceived the research framework and developed the methodology. ZHX was responsible for the code compilation, data analysis, graphic visualization, and first draft writing. FWH managed the implementation of research activities and revised the manuscript. ZH collected data for this study. All authors discussed the results and contributed to the final version of the paper.

**Competing interests.** The authors declare that they have no conflict of interest.

**Special issue statement.** This article is part of the special issue “Advances in flood forecasting and early warning”. It is not associated with a conference.

**Acknowledgements.** This work was mainly supported by the National Key Research and Development Program of China (grant nos. 2018YFC1508803 and 2017YFA0604903), and the Key Special Project for Introduced Talents Team of Southern Marine Science and Engineering Guangdong Laboratory (Guangzhou) (No. GML2019ZD0601). The authors would like to acknowledge Kang Ying and Lin Song of the *Zhejiang Design Institute of Water Conservancy & Hydro-Electric Power* for providing the simulation inundation of flooding model in Liandu District.

**Financial support.** This research has been supported by the National Key Research and Development Program of China (grant nos. 2018YFC1508803 and 2017YFA0604903), and the Key Special Project for Introduced Talents Team of Southern Marine Science and Engineering Guangdong Laboratory (Guangzhou) (grant no. GML2019ZD0601).

## References

- Albano, R., Sole, A., Adamowski, J., Perrone, A. and Inam, A.: Using FloodRisk GIS freeware for uncertainty analysis of direct economic flood damages in Italy, *Int. J. Appl. Earth Obs. Geoinf.*, 73(February), 220–229, doi:10.1016/j.jag.2018.06.019, 2018.
- Alfieri, L., Feyen, L. and Di Baldassarre, G.: Increasing flood risk under climate change: a pan-European assessment of the benefits of four adaptation strategies, *Clim. Change*, 136(3–4), 507–521, doi:10.1007/s10584-016-1641-1, 2016.
- Amadio, M., Mysiak, J., Carrera, L. and Koks, E.: Improving flood damage assessment models in Italy, *Nat. Hazards*, 82(3), 2075–2088, doi:10.1007/s11069-016-2286-0, 2016.



- Büchle, B., Kreibich, H., Kron, A., Thieken, A., Ihringer, J., Oberle, P., Merz, B. and Nestmann, F.: Flood-risk mapping: contributions towards an enhanced assessment of extreme events and associated risks, *Nat. Hazards Earth Syst. Sci.*, 6(4), 483–503, doi:10.5194/nhess-6-485-2006, 2006.
- 325 Cao, S., Fang, W. and Tan, J.: Vulnerability of building contents to coastal flooding based on questionnaire survey in Hainan after typhoon Rammasun and Kalmeagi, *J. Catastrophology*, 31(2), 188–195, doi:https://doi.org/10.3969/j.issn.1000-811X.2016.02.036, 2016.
- Carisi, F., Schröter, K., Domeneghetti, A., Kreibich, H. and Castellarin, A.: Development and assessment of uni- and multivariable flood loss models for Emilia-Romagna (Italy), *Nat. Hazards Earth Syst. Sci.*, 18(7), 2057–2079, doi:10.5194/nhess-18-2057-2018, 2018.
- 330 Coto, E. B.: Flood hazard, vulnerability and risk assessment in the city of Turrialba, Costa Rica, International Institute for Geo-information Science and Earth Observation (ITC), Enschede, The Netherlands. [online] Available from: [http://www.itc.nl/library/Papers/msc\\_2002/ereg/badilla\\_coto.pdf](http://www.itc.nl/library/Papers/msc_2002/ereg/badilla_coto.pdf), 2002.
- Dutta, D., Herath, S. and Musiak, K.: A mathematical model for flood loss estimation, *J. Hydrol.*, 277(1–2), 24–49, doi:10.1016/S0022-1694(03)00084-2, 2003.
- 335 Elkhrachy, I.: Flash Flood Hazard Mapping Using Satellite Images and GIS Tools: A case study of Najran City, Kingdom of Saudi Arabia (KSA), *Egypt. J. Remote Sens. Sp. Sci.*, 18(2), 261–278, doi:10.1016/j.ejrs.2015.06.007, 2015.
- EMA: Disaster loss assessment guidelines, Part III, Emergency management practice, Volume 3, guidelines, Canberra, Emergency Management Australia (EMA), 2002.
- Falter, D., Schröter, K., Dung, N. V., Vorogushyn, S., Kreibich, H., Hundecha, Y., Apel, H. and Merz, B.: Spatially coherent flood risk assessment based on long-term continuous simulation with a coupled model chain, *J. Hydrol.*, 524, 182–193, doi:10.1016/j.jhydrol.2015.02.021, 2015.
- FEMA: Multi-hazard Loss estimation methodology. Flood Model, HAZUS-MH technical manual., 2017.
- Gerl, T., Kreibich, H., Franco, G., Marechal, D. and Schröter, K.: A review of flood loss models as basis for harmonization and benchmarking, *PLoS One*, 11(7), doi:10.1371/journal.pone.0159791, 2016.
- 345 Hasanzadeh Nafari, R., Ngo, T. and Lehman, W.: Calibration and validation of FLFArs-A new flood loss function for Australian residential structures, *Nat. Hazards Earth Syst. Sci.*, 16(1), 15–27, doi:10.5194/nhess-16-15-2016, 2016a.
- Hasanzadeh Nafari, R., Ngo, T. and Lehman, W.: Development and evaluation of FLFAcs - A new Flood Loss Function for Australian commercial structures, *Int. J. Disaster Risk Reduct.*, 17, 13–23, doi:10.1016/j.ijdr.2016.03.007, 2016b.
- 350 Hsu, W.-K., Huang, P.-C., Chang, C.-C., Chen, C.-W., Hung, D.-M. and Chiang, W.-L.: An integrated flood risk assessment model for property insurance industry in Taiwan, *Nat. Hazards*, 58(3), 1295–1309, doi:10.1007/s11069-011-9732-9, 2011.
- Jonkman, S. N., Bočkarjova, M., Kok, M. and Bernardini, P.: Integrated hydrodynamic and economic modelling of flood damage in the Netherlands, *Ecol. Econ.*, 66(1), 77–90, doi:10.1016/j.ecolecon.2007.12.022, 2008.
- Kang, Y. and Chen, Z.: Simulation model of water resources allocation in plain river network area, *Water Resour. Prot.*, 23(5), 31–34+37, doi:https://doi.org/10.3969/j.issn.1004-6933.2007.05.009, 2007.



- 355 Koks, E. E., Jongman, B., Husby, T. G. and Botzen, W. J. W.: Combining hazard, exposure and social vulnerability to provide lessons for flood risk management, *Environ. Sci. Policy*, 47, 42–52, doi:10.1016/j.envsci.2014.10.013, 2015.
- Komolafe, A. A., Herath, S. and Avtar, R.: Development of generalized loss functions for rapid estimation of flood damages: a case study in Kelani River basin, Sri Lanka, *Appl. Geomatics*, 10(1), 13–30, doi:10.1007/s12518-017-0200-4, 2018.
- Li, K., Wu, S., Dai, E. and Xu, Z.: Flood loss analysis and quantitative risk assessment in China, *Nat. Hazards*, 63(2), 737–  
360 760, doi:10.1007/s11069-012-0180-y, 2012.
- Li, N., Zhang, Z., Chen, X. and Feng, J.: Importance of economic loss evaluation in natural hazard and disaster research, *Prog. Geogr.*, 36(2), 256–263, doi:10.18306/dlkxjz.2017.02.011, 2017.
- Limpert, E., Stahel, W. A. and Abbt, M.: Log-normal distributions across the sciences: Keys and clues, *Bioscience*, 51(5), 341–352, doi:10.1641/0006-3568(2001)051[0341:LNDATS]2.0.CO;2, 2001.
- 365 Merz, B., Kreibich, H., Thielen, A. and Schmidtke, R.: Estimation uncertainty of direct monetary flood damage to buildings, *Nat. Hazards Earth Syst. Sci.*, 4(1), 153–163, doi:10.5194/nhess-4-153-2004, 2004.
- Merz, B., Kreibich, H., Schwarze, R. and Thielen, A.: Review article “assessment of economic flood damage,” *Nat. Hazards Earth Syst. Sci.*, 10(8), 1697–1724, doi:10.5194/nhess-10-1697-2010, 2010.
- Mo, W. and Fang, W.: Empirical vulnerability functions of building contents to flood based on post-typhoon (Fitow, 201323)  
370 questionnaire survey in Yuyao, Zhejiang, *Trop. Geogr.*, 36(4), 633-641+657, doi:https://doi.org/10.13284/j.cnki.rddl.002828, 2016.
- NRC: Canadian guidelines and database of flood vulnerability functions, Canada, Natural Resources Canada, Public Safety Canada., 2017.
- Penning-Rowsell, E. C., Yanyan, W., Watkinson, A. R., Jiang, J. and Thorne, C.: Socioeconomic scenarios and flood damage  
375 assessment methodologies for the Taihu Basin, China, *J. Flood Risk Manag.*, 6(1), 23–32, doi:10.1111/j.1753-318X.2012.01168.x, 2013.
- Qie, Z. and Rong, L.: An integrated relative risk assessment model for urban disaster loss in view of disaster system theory, *Nat. Hazards*, 88(1), 165–190, doi:10.1007/s11069-017-2861-z, 2017.
- Reese, S. and Ramsay, D.: RiskScape: Flood fragility methodology, Wellington: New Zealand Climate Change Research  
380 Institute., 2010.
- Scawthorn, C., Asce, F., Flores, P., Blais, N., Seligson, H., Tate, E., Chang, S., Mifflin, E., Thomas, W., Murphy, J., Jones, C. and Lawrence, M.: HAZUS-MH Flood Loss Estimation Methodology. II. Damage and Loss Assessment, *Nat. Hazards Rev.*, 7(2), 72–81, doi:10.1061/ASCE1527-698820067:272, 2006.
- Shen, Y., Zhao, P., Pan, Y. and Yu, J.: A high spatiotemporal gauge-satellite merged precipitation analysis over China, *J. Geophys. Res. Atmos.*, 119, 3063–3075, doi:https://doi.org/10.1002/2013JD020686, 2014.
- 385 Shi, Y.: Research on vulnerability assessment of cities on the disaster scenario: A case study of Shanghai city, East China Normal University, Shanghai, China., 2010.



- Smith D: Flood damage estimation A review of urban stage damage curves and loss functions, *Water SA*, 20(3), 231–238, 1994.
- 390 Stephenson, V. and D’Ayala, D.: A new approach to flood loss estimation and vulnerability assessment for historic buildings in England, *Nat. Hazards Earth Syst. Sci. Discuss.*, 1(5), 6025–6060, doi:10.5194/nhessd-1-6025-2013, 2013.
- UNISDR: The Pocket GAR 2015 Making Development Sustainable: The Future of Disaster Risk Management, Geneva, Switzerland: United Nations Office for Disaster Risk Reduction (UNISDR)., 2015.
- Wehner, M., Canterford, S., Corby, N., Edwards, M. and Juskevics, V.: Vulnerability of Australian houses to riverine  
395 inundation: analytical and empirical vulnerability curves, Canberra: Geoscience Australia., 2017.
- Zhao, Y., Gong, Z., Wang, W. and Luo, K.: The comprehensive risk evaluation on rainstorm and flood disaster losses in China mainland from 2004 to 2009: Based on the triangular gray correlation theory, *Nat. Hazards*, 71(2), 1001–1016, doi:10.1007/s11069-013-0698-7, 2014.
- Zhou, Y., Lu, G., Jin, J., Tong, F. and Zhou, P.: A high precision comprehensive evaluation method for flood disaster loss  
400 based on improved genetic programming, *J. Ocean Univ. China*, 5(4), 322–326, doi:10.1007/s11802-006-0023-0, 2006.